Histol Histopathol (2022) 37: 879-888

**http://www.hh.um.es**

Histology and Histopathology
*From Cell Biology to Tissue Engineering*

**ORIGINAL ARTICLE** **Open Access**

# MiR-129-5p/TRIP13 affects malignant phenotypes of colorectal cancer cells

**Yongqing Cao, Fang Huang, Jiheng Liu, Hui Qi and Jinjun Xiao**

Department of Hematology, The First Hospital of Changsha, Changsha City, Hunan Province, China

**Summary.** Objective. Aberrant miR-129-5p expression is a key modulator of cancer development. But how the miRNA affects colorectal cancer (CRC) remains unclear. This study was designed to illustrate the underlying mechanism of miR-129-5p in CRC.

Methods. MiR-129-5p expression at cellular level was assayed by qRT-PCR. Its role in CRC cell phenotypes was studied by cell function experiments. The binding relationship between miR-129-5p and TRIP13 was analyzed and verified by bioinformatics prediction and dual-luciferase detection. Furthermore, the functional mechanism based on miR-129-5p and TRIP13 in CRC was studied through rescue experiments.

Results. CRC cell lines presented prominently lower miR-129-5p levels than the normal colon epithelial cell line. The forced miR-129-5p level suppressed CRC cell growth. TRIP13 was proved to be a target of miR-129-5p in CRC cells, and miR-129-5p overexpression reduced TRIP13 expression. TRIP13 knockdown resulted in cell cycle arrest. Additionally, TRIP13 overexpression restored the impacts of miR-129-5p overexpression on cell malignant phenotypes and cell cycle.

Conclusion. MiR-129-5p down-regulated TRIP13 expression, thereby restraining the malignant progression of CRC cells. The findings may offer a new target for molecular therapy of CRC.

**Key words:** miR-129-5p, TRIP13, Colorectal cancer, Malignant phenotype

## Introduction

Colorectal cancer (CRC) is a frequent and deadly malignancy throughout the world, and it is one major cause of cancer death in China (Mauri et al., 2019). In 2018, there were 1.8 million new cases of CRC, resulting in 881,000 deaths (Bray et al., 2018). Recurrence and metastasis lead to high mortality of CRC, but its underlying molecular mechanisms remain elusive.

Mechanically, microRNAs (miRNAs) bind to the complementary sites on the 3'-untranslated region (3'-UTR) and suppress the expression of target genes (Lu and Rothenberg, 2018; Correia de Sousa et al., 2019). MiRNAs can modulate many biological processes, like cell movement, cell proliferation, and cell death (Mishra et al., 2016; Rupaimoole and Slack, 2017). Evidence has demonstrated that dysregulation of miRNA can affect the progression of cancer (Kristensen et al., 2019; Takahashi et al., 2019). Many miRNAs were proved to be oncogenes or suppressors in tumor. For example, miR-145-5p serves as a tumor inhibitor in prostate cancer by mediating tumor-related behaviors of cancer cells via modulating SENP1 (He et al., 2018). MiR-129-5p affects apoptosis and proliferation of CRC cells (Wu et al., 2018). PITPNA-AS1 can accelerate migration and proliferation, and inhibit apoptosis of CRC cells via the miR-129-5p/HMGB1 axis (Yuan and Yang, 2020). LncRNA HIF1A-AS2 positively affects colorectal cancer development and epithelial-mesenchymal transition (EMT) by regulating miR-129-5p and DNMT3A (Lin et al., 2018). However, the molecular mechanisms by which miR-129-5p influences CRC development remain unexplored.

TRIP13 exerts a vital function in regulating mitotic processes (Vader, 2015; Lu et al., 2019a,b). TRIP13 is an important gene associated with CIN in human tumors (Zhang et al., 2019). The carcinogenic effects of TRIP13 have become a research focus in recent years. However, the mechanism of TRIP13 in CRC awaits investigation.

Therefore, this work analyzed the modulatory mechanisms of miR-129-5p/TRIP13 axis and explains how they affect the malignant phenotypes of CRC cells. The mechanisms of miR-129-5p and TRIP13 in CRC were analyzed at both molecular and cellular levels. The results suggested that miR-129-5p acted as a tumor inhibitor in CRC. Moreover, miR-129-5p blocked growth, movement, and cell cycle progression of CRC cells via modulating TRIP13.

*Corresponding Author:* Yongqing Cao, Department of Hematology, The First Hospital of Changsha, 311 Camp Pan Road, Kaifu District, Changsha City, Hunan Province, China, 410005. e-mail: YongqingCao2021@163.com

DOI: 10.14670/HH-18-455

## Materials and methods

### *Bioinformatics methods*

From The Cancer Genome Atlas (TCGA), mature miRNA expression data and mRNA sequencing data of CRC (TCGA-COAD&READ) were downloaded. In differential analysis, miRNA data included 603 cancer tissue samples and 11 normal tissue samples. The mRNA sequencing data included 625 cancer tissue samples and 51 normal tissue samples. With |logFC|>2 and adj. pvalue<0.05 as standards, differential miRNAs and mRNAs were obtained, and target miRNA of the study was determined. Downstream targets of miR-129-5p were predicted with mirDIP, miRWalk, miRDB and starBase databases. The obtained mRNAs were overlapped with the differentially up-regulated mRNAs. In this way we obtained one target gene, TRIP13. Then, we identified the correlation between TRIP13 and miR-129-5p. Gene Set Enrichment Analysis (GSEA) software was applied for pathway enrichment analysis.

### *Cell culture*

Human CRC cell lines Caco-2 (BNCC102170), LoVo (BNCC338601), HT29 (BNCC100164), SW480 (BNCC100604), SW620 (BNCC100162) and human normal colon epithelial cell line NCM460 (BNCC339288) were all from BeNa culture collection (BNCC, China). All of them were incubated in DMEM (Sigma, USA) with 10% FBS (Hyclone, USA) at 37°C with 5% $CO_2$.

### *Cell transfection*

MiR-129-5p mimic, miR-129-5p inhibitor, over expression-TRIP13 (oe-TRIP13), short hairpin-TRIP13 (sh-TRIP13), mimic negative control (mimic NC), inhibitor NC, oe-NC and sh-NC, obtained from Sangon Biotech (Shanghai, China), were subcloned into SW480 and HT29 cell lines with Lipofectamine 2000 (Thermo Fisher Scientific, Inc., USA). After 4 h, the medium without FBS was changed with complete medium with 10% FBS, and cells were kept for 48 h for later use.

**Table 1.** qRT-PCR primer sequence.

| Target gene | Primer (5'-3') |
|---|---|
| miR-129-5p | F: 5'- CGGCGGTTTTTTGCGGTCTGGGCT-3'<br>R: 5'- AGCCCAGACCGCAAAAAACCGCCG-3' |
| U6 | F: 5'-CTCGCTTCGGCAGCACA-3'<br>R: 5'-AACGCTTCACGAATTTGCGT-3' |
| TRIP13 | F: 5'- GTAAAGCGTTAGCCCAGAAA-3'<br>R: 5'- CAATCAGCACGAACACCAG-3' |
| GAPDH | F: 5'-GATTCCTATGTGGGCGACGAG-3'<br>R: 5'-CCATCTCTTGCTCGAAGTCC-3' |

### *qRT-PCR*

Trizol Reagent (Invitrogen, USA) was utilized to isolate total RNA. Then, complementary DNA was synthesized using PrimeScript RT Reagent Kit (Takara, RR047A, China). Table 1 lists the primer sequences. qRT-PCR was carried out by using SYBR Prime Script RT-PCR Kits (Takara). The conditions for reaction were: 95°C for 10 min and 35 cycles of 95°C for 10 s, 57°C for 30 s and 72°C for 30 s. The data were normalized to U6 or GAPDH and calculated by $2^{-\Delta\Delta CT}$ method.

### *Western blot*

RIPA reagent (Beyotime, China) was introduced to isolate total proteins 48 h after cell transfection. Protein samples were loaded and isolated by 10% SDS-PAGE, and then transferred to a PVDF membrane. Next, the membrane was blocked with 5% skimmed milk and washed with TBST. Afterward, it was reacted with anti-TRIP13 (1:500, ab64964, abcam, UK) and anti-GAPDH (1:10000, ab181602, abcam, UK). Thereafter, the membrane was washed 3 times with TBST. Subsequently, it was incubated with horseradish peroxidase conjugated second antibody (Beyotime). Finally, images were developed with an optical luminescence instrument (GE, USA) and photographed.

### *CCK-8 and colony formation detections*

CCK-8 assay was introduced to analyze cell viability. Cells were inoculated in 96-well plates, mixed with 10 μL CCK-8 reagent, and cultured for 2 h for 4 consecutive days. The cells were incubated at the same time every day. The absorbance was detected at 450 nm to reflect cell proliferative activity.

To assess the colony formation of cells, 500 treated cells were planted into a 6-well plate. Every 3 days, the medium was changed. When the cell colonies were visible, the medium was discarded. Then, the wells were washed with phosphate buffer saline (PBS). Next, the cell fixing and staining were performed with 4% paraformaldehyde (Sigma-Aldrich, USA) and 0.5% crystal violet (Sigma-Aldrich, USA), respectively. After the cell colonies were dried, photos were taken and cell colonies were counted.

### *Dual-luciferase reporter assay*

Target fragment was inserted into the luciferase vector pmiRGLO (Promega, USA) using T4 DNA ligase to construct luciferase reporter plasmids wild-type (WT)-TRIP13 and mutant (MUT)-TRIP13, with the following corresponding sequences on 3'UTR: WT-TRIP13: 5'-CGUUUGAUUUAGUGCAAAAAU-3'; MUT-TRIP13: 5'-CUUUCGGUUGGAUUACGCAAA -3'. WT-TRIP13 was co-transfected with mimic NC or miR-129-5p mimic into the cells, also the same treatment was conducted with swapping WT-TRIP13 to

MUT-TRIP13. After incubation for 48 h, cells were collected. Luciferase intensity was evaluated by Promega (Madison, USA).

### Transwell assay

After transfection, the cells were placed in medium without serum for 12 h. After that, cells were gathered and resuspended in the medium added with 0.2% FBS. The invasion assay employed a 24-well Transwell device (8-μm pore size, USA), which was pretreated with Matrigel (BD Biosciences, USA). The upper chamber of the device was injected with cell suspension (100 μL, $5\times10^4$ cells), while the lower chamber was added with 500 μL medium with 10% FBS. After 24 h, the cells which failed to invade were removed, and the invasive cells were fixed with paraformaldehyde for 20-30 min. Subsequently, the cells were washed, dyed with 0.1% crystal violet for 30 min, and then washed again. Finally, the invasive cells were observed under a microscope.

### Scratch healing assay

First, horizontal lines were evenly plotted on the back of a 6-well plate with a marker. Then, cells ($2.5\times10^5$ cells/mL) were added to each well. When cell monolayer formed, a straight wound was created using a sterilized white pipette (10 μL). Then, 1×PBS was used to wash off the dropped cells. The remaining cells were kept in medium without FBS for 48 h and photographed under a microscope to calculate the cell migration rate.

### Flow cytometry

The cells were gathered, rinsed two times with cold PBS, and fixed with cold 75% ethanol at 4°C overnight.

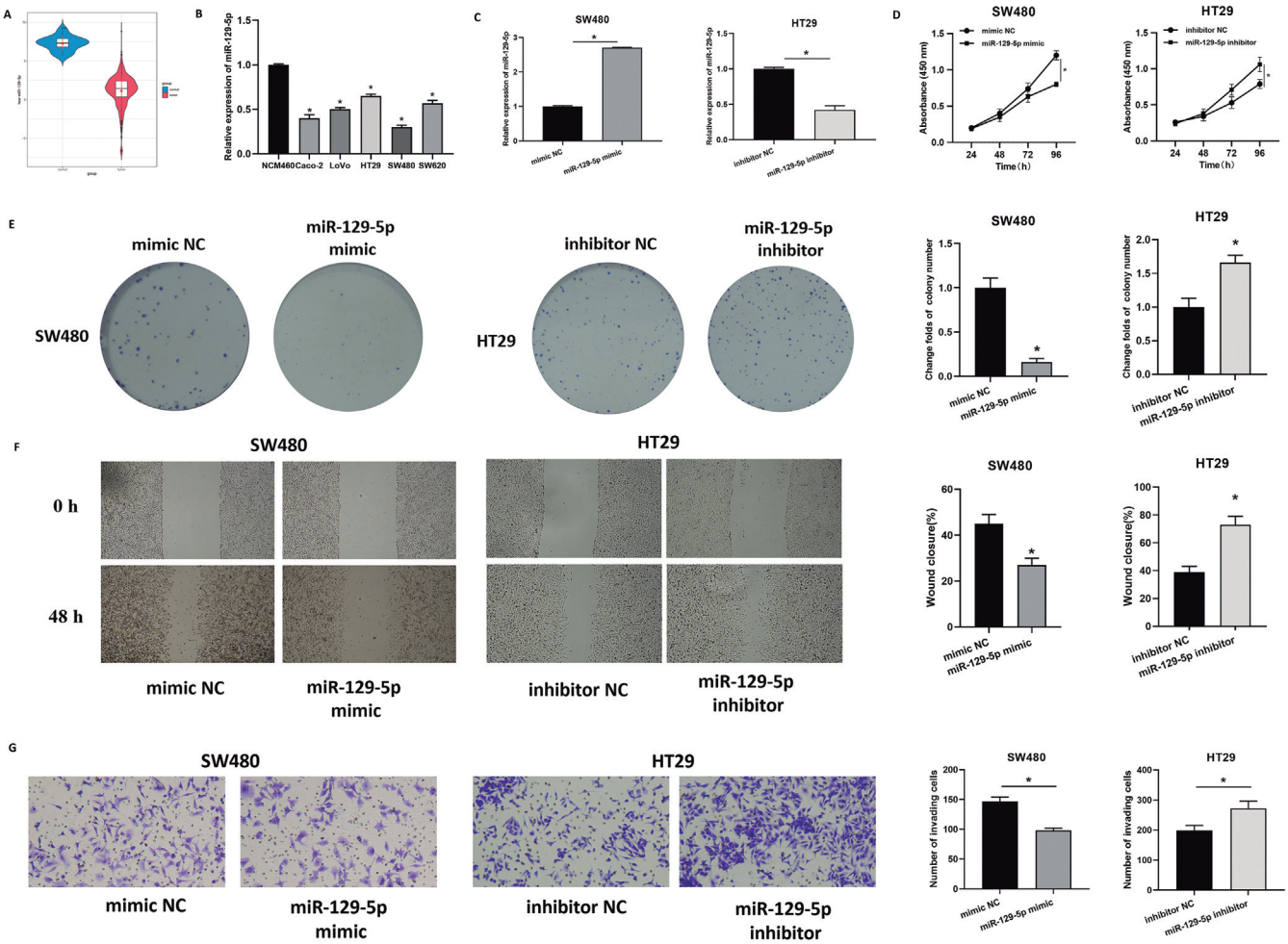


**Fig. 1.** MiR-129-5p restrains malignant cell behaviors in CRC. **A.** Differential expression of miR-129-5p in CRC tissue samples (blue for normal, red for tumor). **B.** MiR-129-5p expression in human normal colon epithelial cell line NCM460 and CRC cell lines Caco-2, LoVo, HT29, SW480, SW620. **C.** MiR-129-5p expression in transfected SW480 and HT29 cells. **D.** The cell viability of SW480 and HT29 cells transfected with miR-129-5p mimic or miR-129-5p inhibitor. **E.** The colony formation of transfected cells. **F.** The migration of transfected cells. **G.** The invasion of transfected cells. * $p<0.05$. F, x 40; G, x 100.

Next, cells were washed two times with PBS, resuspended, and cultured with RNase for 30 min. Next, cells were dyed with 0.5 mL propidium iodide (50 μg/mL) in darkness for 30 min at room temperature. The last step was to analyze cell cycle with FACSCalibur flow cytometry (BD Biosciences, USA).

### *Data analysis*

Data were handled by GraphPad Prism 8 (GraphPad Software Inc., USA). Measurement data are shown as mean ± standard deviation. The inter-group comparison was conducted with t-test. $P<0.05$ indicates a prominent difference.

## Results

### *MiR-129-5p restrains proliferation, migration and invasion of CRC cells*

To explore dysregulated miRNA in CRC, we obtained mature miRNA expression profiles from TCGA-COAD&READ dataset and uncovered that miR-129-5p was notably suppressed in CRC (Fig. 1A). To verify bioinformatics analysis results, qRT-PCR was conducted and revealed that compared with normal colon epithelial cell line NCM460, all CRC cell lines (Caco-2, LoVo, HT29, SW480 and SW620) showed notably reduced miR-129-5p level, with the lowest in SW480 and the highest in HT29 (Fig. 1B). Therefore, SW480 and HT29 were chosen for further cell function study.

MiR-129-5p mimic/inhibitor was then transfected into SW480 and HT29 cells. The result of qRT-PCR indicated successful transfection (Fig. 1C). CCK-8 result revealed that miR-129-5p high level prominently repressed growth of SW480 cells (Fig. 1D). Colony formation test indicated that miR-129-5p mimic reduced the colony number of SW480 cells (Fig. 1E). On the contrary, inhibition of miR-129-5p expression boosted proliferation of HT29 and SW480 cells (Fig. 5A-C).

According to the scratch healing test data, miR-129-5p forced expression notably impeded migration of transfected cells. Moreover, Transwell assay displayed that miR-129-5p high expression weakened invasion of CRC cells compared with the control group, while its inhibition produced the inverse effect (Fig. 1F,G, 5D,E).

Collectively, miR-129-5p hampered malignant progression of CRC cells.

### *TRIP13 exhibits high expression in CRC and is targeted by miR-129-5p*

To further study the downstream modulatory mechanism of miR-129-5p, mRNA expression data in CRC tissues were downloaded from TCGA-COAD&READ database in this study. Through differential analysis, we obtained a total of 2,080

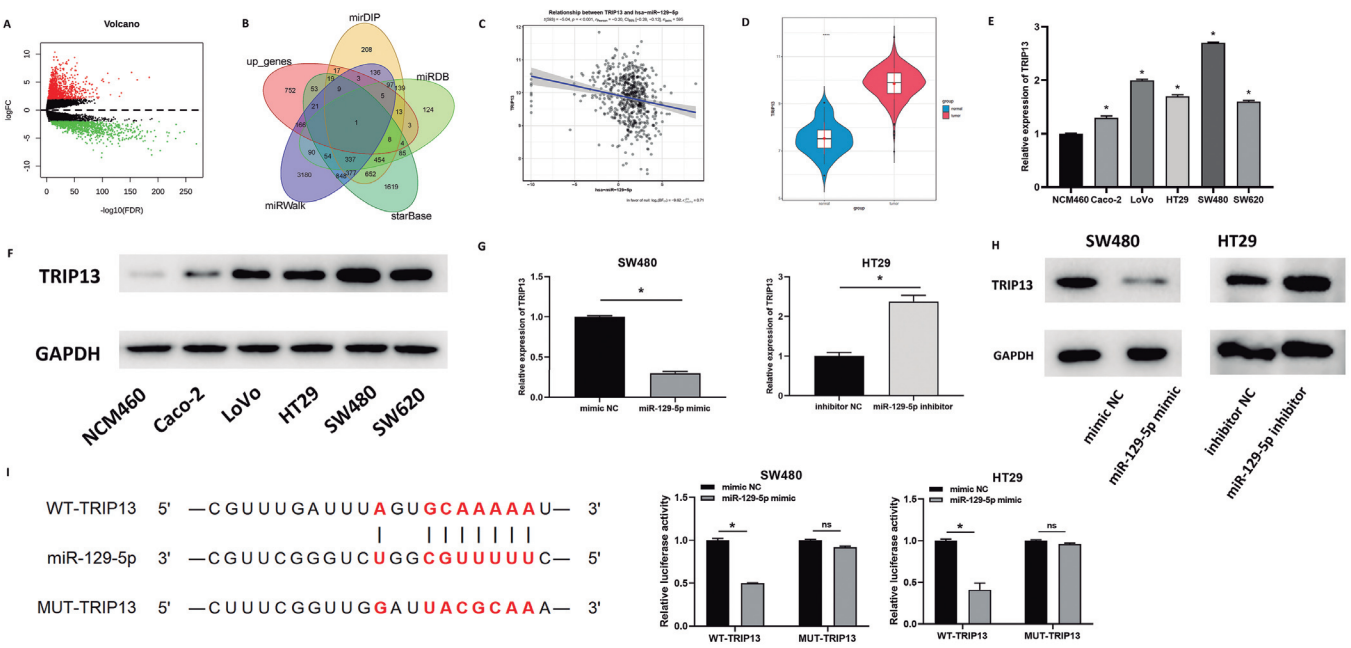


**Fig. 2.** TRIP13 is targeted by miR-129-5p. **A.** Volcano plot of differential analysis on mRNAs (red and green represent upregulation and downregulation, respectively). **B.** Venn diagram of predicted targets and differentially upregulated mRNAs. **C.** Correlation between TRIP13 and miR-129-5p. **D.** Violinplot of TRIP13 expression (blue represents normal, red represents tumor). **E, F.** TRIP13 mRNA and protein levels in different cell lines. **G, H.** Effect of overexpressed/inhibited miR-129-5p on TRIP13 mRNA and protein levels. **I.** Targeted binding of miR-129-5p to TRIP13; * $p<0.05$.

differential mRNAs, among which 1,074 were downregulated and 1,006 were upregulated (Fig. 2A). The targets of miR-129-5p were predicted by employing StarBase, miRDB, mirDIP and miRWalk databases. The obtained genes were overlapped with the differentially upregulated mRNAs, and finally one target gene (TRIP13) was obtained (Fig. 2B). The negative correlation between TRIP13 and miR-129-5p was indicated by correlation analysis (Fig. 2C). TRIP13 was overexpressed in CRC tissues (Fig. 2D). Through qRT-PCR, we also uncovered that TRIP13 was at high expression level in CRC cell lines compared to NCM460 (Fig. 2E). Western blot was introduced to demonstrate protein expression, which was in accordance with the PCR result (Fig. 2F). In conclusion, TRIP13 level was stimulated in CRC.

In SW480 cells, upregulation of miR-129-5p reduced TRIP13 mRNA level, while downregulation had the opposite effects in SW480 and HT29 cells (Fig. 2G, 5F). Besides, Western blot displayed that TRIP13 protein expression was lowered by miR-129-5p mimic and increased by miR-129-5p inhibitor (Figs. 2H, 5G). Through starBase, a complementary site between the 3'-UTR sequence of TRIP13 mRNA and miR-129-5p was discovered (Fig. 2I). Then dual-luciferase detection was performed. As expected, relative luciferase intensity of cells with miR-129-5p mimic and WT-TRIP13 was reduced (Fig. 2I). Hence, miR-129-5p may hinder CRC progression by modulating TRIP13.

### *TRIP13 affects the cell cycle of CRC cells*

TRIP13 expresses highly in CRC cell lines, which can facilitate the invasion of cancer cells and are associated with poor prognosis of CRC (Kurita et al., 2016; Sheng et al., 2018). The results of GSEA pathway enrichment analysis displayed that TRIP13 was markedly gathered in cell cycle-related pathways and p53 signaling pathway (Fig. 3A). Hence, this study mainly explored the influence of TRIP13 on cell cycle changes. Subsequently, sh-TRIP13 and oe-TRIP13 were used to inhibit and induce the expression of TRIP13, respectively. qRT-PCR and western blot validated the transfection efficiency (Fig. 3B,C, 6A,B). Later, the influence of TRIP13 on cell cycle was verified by flow cytometry, and the results demonstrated that TRIP13

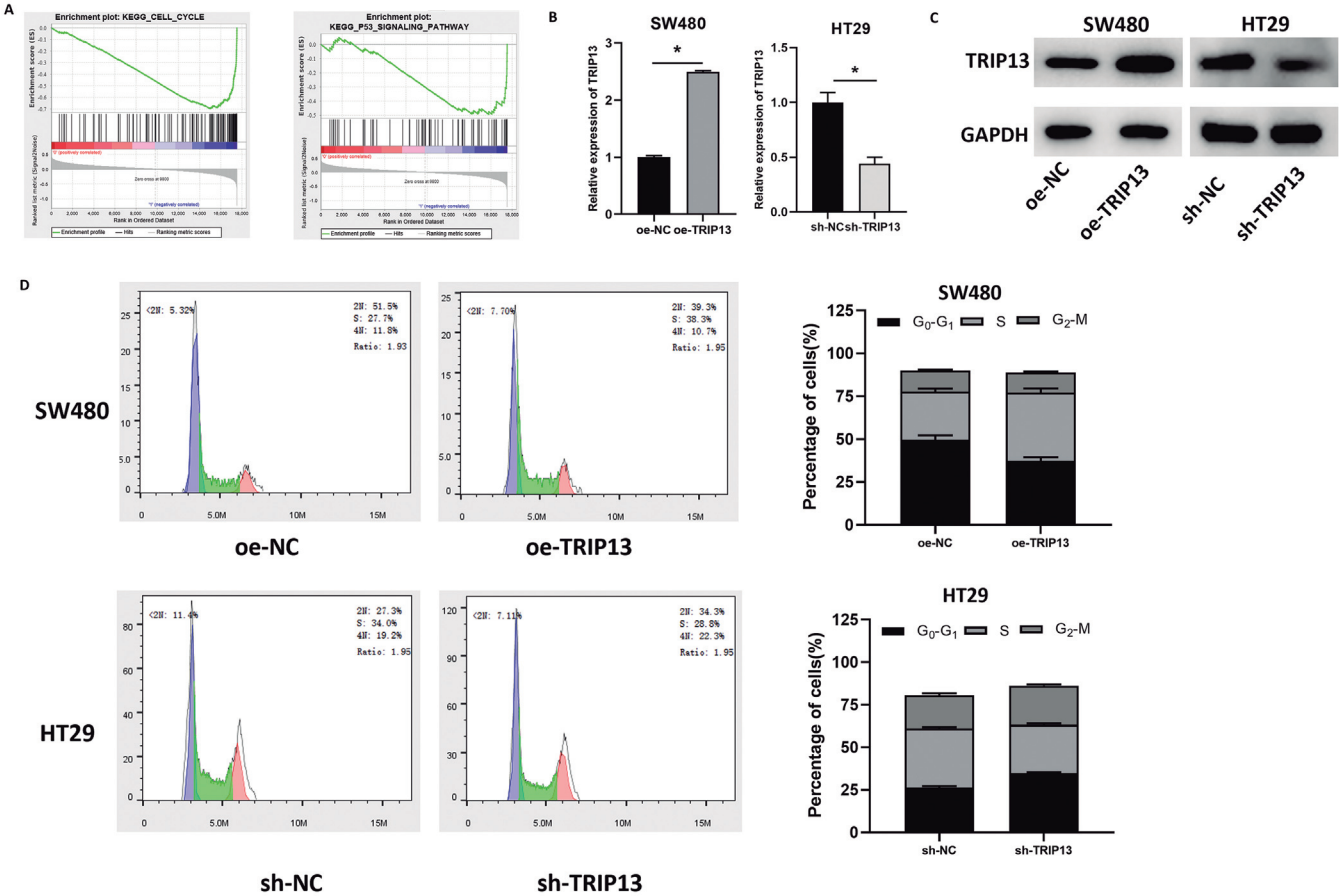


**Fig. 3.** TRIP13 influences cell cycle of CRC cells. **A.** GSEA enrichment analysis results of TRIP13. **B, C.** TRIP13 mRNA and protein levels in oe-NC, oe-TRIP13, sh-NC and sh-TRIP13 groups. **D.** The effect of overexpressed/silenced TRIP13 on cell cycle; * $p<0.05$.

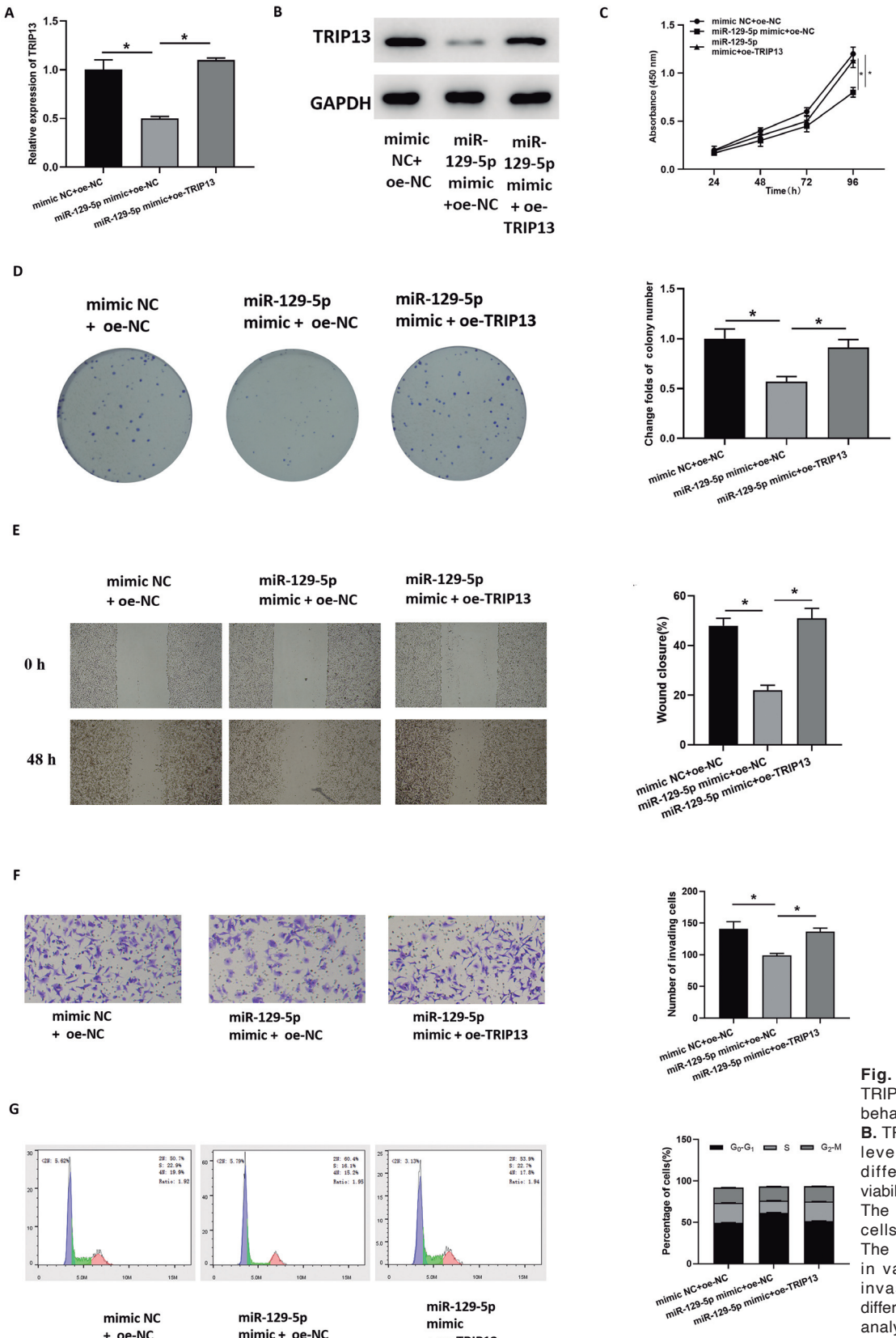


**Fig. 4.** MiR-129-5p targets TRIP13 and affects malignant behaviors of CRC cells . **A, B.** TRIP13 mRNA and protein levels in SW480 cells in different groups. **C.** Cell viability in varying groups. **D.** The colony forming ability of cells in varying groups. **E.** The migratory ability of cells in varying groups. **F.** The invasive ability of cells in different groups. **G.** Cell cycle analysis in different groups; * p<0.05. E, x 40; F, x 100.

knockdown resulted in cell cycle arrest in G1 phase, and TRIP13 overexpression showed the opposite effect (Fig. 3D, 6C).

### *TRIP13 overexpression reverses the repressive role of miR-129-5p mimic on SW480 cell progression*

To verify whether TRIP13 is critical for the function of miR-129-5p in CRC cells, rescue experiments were performed. qRT-PCR and western blot revealed that miR-129-5p mimic suppressed TRIP13 mRNA and protein expression, and this effect was reversed by oe-TRIP13 transfection (Fig. 4A,B). In the CCK-8 assay, TRIP13 overexpression reversed the suppressive role of miR-129-5p mimic on SW480 cell growth (Fig. 4C). Colony formation assay stated that TRIP13 overexpression increased the colony number, which was decreased with miR-129-5p mimic (Fig. 4D). Both scratch healing and the Transwell assays suggested that cell migration and invasion were prominently reduced by miR-129-5p mimic, while they recovered upon the overexpression of TRIP13 (Fig. 4E,F). Flow cytometry result displayed that TRIP13 overexpression notably reduced the blocking role of miR-129-5p overexpression on the cell cycle (Fig. 4G). Altogether, miR-129-5p targeted TRIP13 and hindered the malignant progression of CRC cells.

## Discussion

More and more investigations have reported that miRNA can influence gene expression, and it is crucial for many biological progresses (Tiwari et al., 2018). Currently, the oncogenic or anticancer effects of various miRNAs in different tumors have been reported, including the miR-129 family.

MiR-129-2-3p, miR-129-1-3p and miR-129-5p are 3 mature miRNAs in the miR-129 familiy (Lu et al., 2018). MiR-129 expression is inhibited in many cancers, like medulloblastoma, gastric cancer, lung adenocarcinoma and bladder cancer (Fesler et al., 2014; Gao et al., 2016; Setijono et al., 2018). MiR-129-5p level is reduced in CRC cells (Wu et al., 2018), and treatment with miR-129-5p inhibitor promotes cell

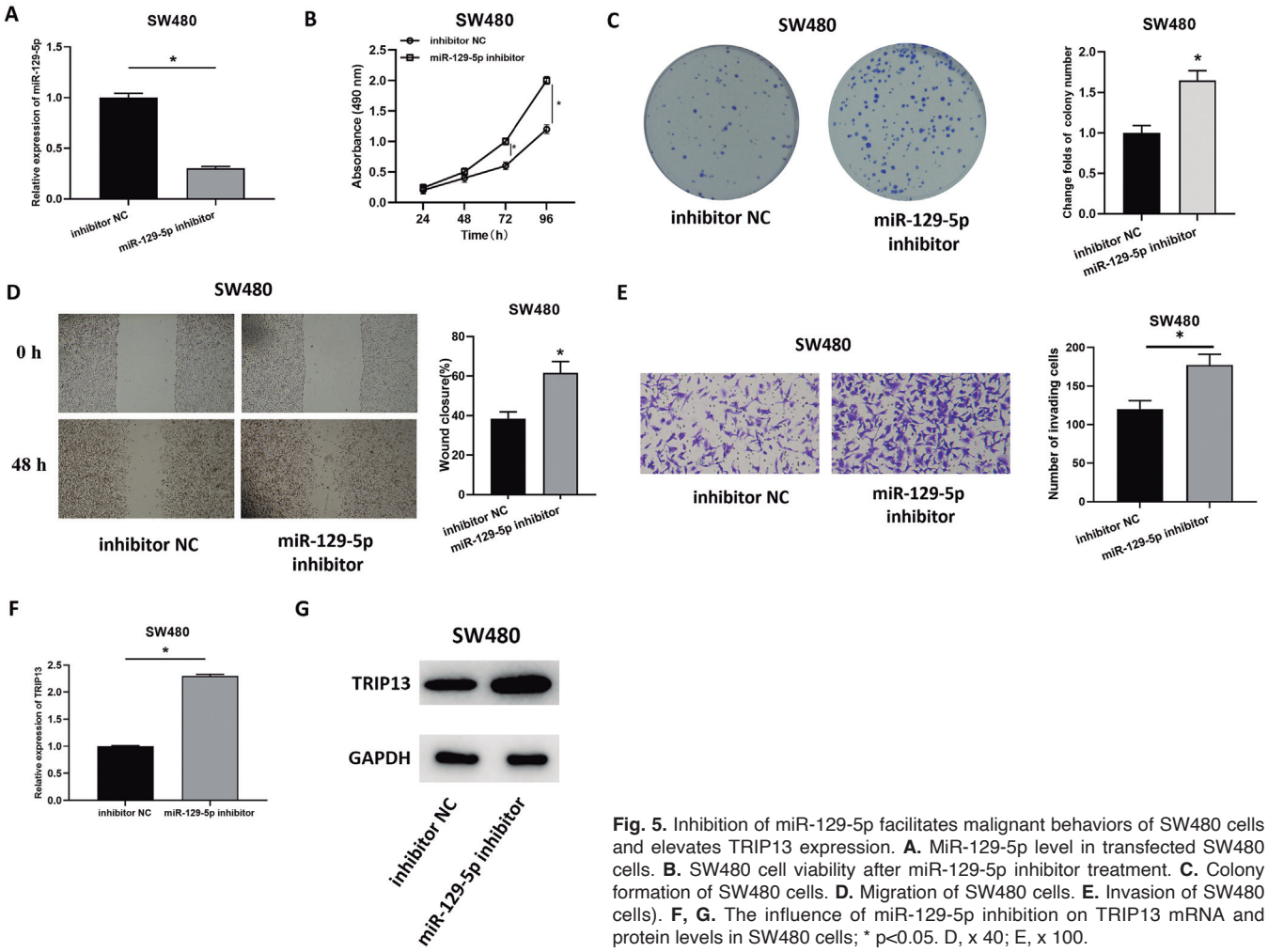


**Fig. 5.** Inhibition of miR-129-5p facilitates malignant behaviors of SW480 cells and elevates TRIP13 expression. **A.** MiR-129-5p level in transfected SW480 cells. **B.** SW480 cell viability after miR-129-5p inhibitor treatment. **C.** Colony formation of SW480 cells. **D.** Migration of SW480 cells. **E.** Invasion of SW480 cells). **F, G.** The influence of miR-129-5p inhibition on TRIP13 mRNA and protein levels in SW480 cells; * $p<0.05$. D, x 40; E, x 100.

proliferation, migration, and apoptosis (Yuan and Yang, 2020). Consistent with previous findings, TCGA data analysis in the present study found that 301 cases of CRC tissues showed low level of miR-129-5p. *In vitro* validation showed that miR-129-5p was downregulated in CRC cells, in which SW480 and HT29 had the lowest and highest miR-129-5p levels, respectively, and they were utilized for further cell function studies. Next, we evaluated the correlation between different clinicopathological features and miR-129-5p expression in TCGA dataset. The results demonstrated that miR-129-5p expression was linked with clinical stage, tumor size and lymph node metastasis (Fig. 7A-C). In addition, *in vitro* experiments also uncovered that miR-129-5p high level hampered malignant progression of SW480 cells. These data manifested the repressive role of miR-129-5p in CRC.

To explore the molecular mechanism of miR-129-5p

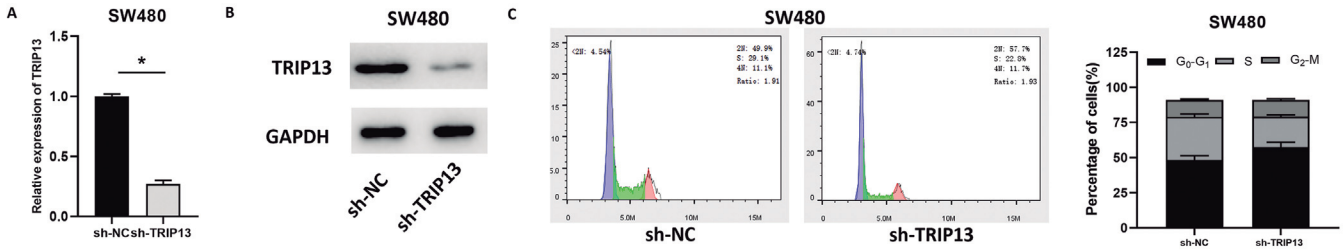


**Fig. 6.** TRIP13 inhibition affects cell cycle of SW480 cells. **A.** TRIP13 expression level in sh-NC and sh-TRIP13 groups. **B.** TRIP13 expression in SW480 cells in different treatment groups. **C.** Effect of TRIP13 silencing on cell cycle of SW480 cells; * p<0.05.

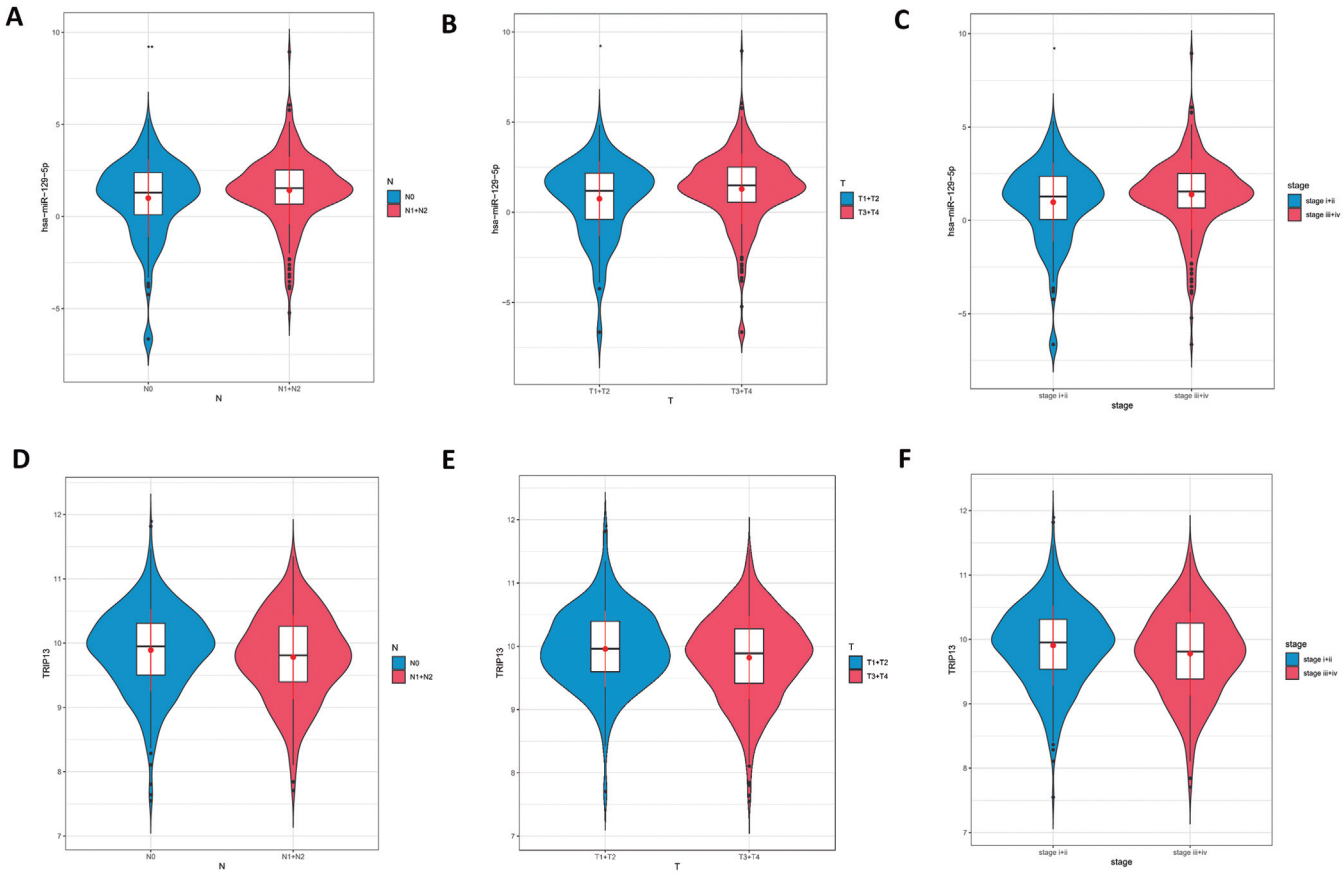


**Fig. 7.** Correlation of miR-129-5p and TRIP13 expression with different clinical features. **A-C.** Correlation between miR-129-5p expression and N stage, T stage, and M stage of CRC patients. **D-F.** Correlation between TRIP13 expression and N stage, T stage, and M stage of CRC patients; * p<0.05, ** p<0.01.

in CRC, its target (TRIP13) was predicted by bioinformatics methods. Firstly, qRT-PCR and western blot were applied to confirm the upregulation of TRIP13 in CRC cells. Subsequently, correlation between TRIP13 and miR-129-5p was detected by dual-luciferase detection, and TRIP13 was a target of miR-129-5p in CRC. TRIP13, located at 5p15.33, participates in some cellular processes, including DNA break repair and recombination, and cell cycle checkpoint signaling (Banerjee et al., 2014; Alfieri et al., 2018). Cell cycle progression is closely linked with the progression of cancer. One recent study shows that TRIP13 affects progression of bladder cancer by regulating the cell cycle (Lu et al., 2019a,b). TRIP13 knockdown blocks lung cancer cells in G2/M phase and regulates gene expression levels associated with cell cycle checkpoints (Zhang et al., 2019a,b). TRIP13 also promotes cell cycle progression in HeLa and breast cancer cells (Eytan et al., 2014; Wang et al., 2014). Similarly, in the present study, GSEA results showed that TRIP13 was remarkably gathered in the pathways involved in the cell cycle. Flow cytometry showed that TRIP13 knockdown blocked cell cycle progression, indicating that TRIP13 facilitated the growth of CRC cells and thus accelerated the cells to entry into mitosis. TRIP13 is boosted in various cancers to promote cell malignant behaviors. For example, TRIP13, as an oncogene, could promote the malignant behaviors of prostate cancer cells by regulating YWHAZ and EMT-related genes (Dong et al., 2019). TRIP13 facilitates the progression of epithelial ovarian cancer via regulating the Notch signaling pathway (Zhou et al., 2019). Through bioinformatics methods, we discovered that TRIP13 level was boosted in 612 CRC tissues, and the abnormal TRIP13 expression had a close relation with clinical stage, tumor size and lymph node metastasis (Fig. 7D-F). These conclusions suggested that abnormally expressed TRIP13 may be related to CRC progression. Herein, it was also proved that overexpressed TRIP13 markedly reduced the inhibitory role of miR-129-5p overexpression on malignant progression of SW480 cells. Therefore, miR-129-5p played its biological function by targeting TRIP13.

Collectively, this work gives new proof for the vital role of miRNA in CRC progression, and also offers a theoretical basis for searching into new targets for CRC treatment and diagnosis.

*Acknowledgements.* Not applicable.

*Ethics approval and consent to participate.* Our study did not require an ethical board approval because it did not contain human or animal trials.

*Consent for publication.* Not applicable.

*Availability of data and materials.* Please contact corresponding author with reasonable request for the original experimental data and materials.

*Competing interest.* The authors declare no conflicts of interest.

*Funding.* Scientific Research Project of Hunan Provincial Health Commission (202203102946).

*Authors' contributions.* All authors contributed to data analysis, drafting and revising the article, gave final approval of the version to be published, and agreed to be accountable for all aspects of the work.

## References

Alfieri C., Chang L. and Barford D. (2018). Mechanism for remodelling of the cell cycle checkpoint protein MAD2 by the ATPase TRIP13. Nature 559, 274-278.

Banerjee R., Russo N., Liu M., Basrur V., Bellile E., Palanisamy N., Scanlon C.S., van Tubergen E., Inglehart R.C., Metwally T., Mani R.S., Yocum A., Nyati M.K., Castilho R.M., Varambally S., Chinnaiyan A.M. and D'Silva N.J. (2014). TRIP13 promotes error-prone nonhomologous end joining and induces chemoresistance in head and neck cancer. Nat. Commun. 5, 4527.

Bray F., Ferlay J., Soerjomataram I., Siegel R.L., Torre L.A. and Jemal A. (2018). Global cancer statistics 2018: GLOBOCAN estimates of incidence and mortality worldwide for 36 cancers in 185 countries. CA Cancer J. Clin. 68, 394-424.

Correia de Sousa M., Gjorgjieva M., Dolicka D., Sobolewski C. and Foti M. (2019). Deciphering miRNAs' action through miRNA editing. Int. J. Mol. Sci. 20, 6249.

Dong L., Ding H., Li Y., Xue D., Li Z., Liu Y., Zhang T., Zhou J. and Wang P. (2019). TRIP13 is a predictor for poor prognosis and regulates cell proliferation, migration and invasion in prostate cancer. Int. J. Biol. Macromol. 121, 200-206.

Eytan E., Wang K., Miniowitz-Shemtov S., Sitry-Shevah D., Kaisari S., Yen T.J., Liu S.T. and Hershko A. (2014). Disassembly of mitotic checkpoint complexes by the joint action of the AAA-ATPase TRIP13 and p31(comet). Proc. Natl. Acad. Sci. USA 111, 12019-12024.

Fesler A., Zhai H. and Ju J. (2014). miR-129 as a novel therapeutic target and biomarker in gastrointestinal cancer. Onco. Targets Ther. 7, 1481-1485.

Gao Y., Feng B., Han S., Lu L., Chen Y., Chu X., Wang R. and Chen L. (2016). MicroRNA-129 in human cancers: from tumorigenesis to clinical treatment. Cell Physiol. Biochem. 39, 2186-2202.

He J.H., Han Z.P., Zhou J.B., Chen W.M., Lv Y.B., He M.L. and Li Y.G. (2018). MiR-145 affected the circular RNA expression in prostate cancer LNCaP cells. J. Cell Biochem. 119, 9168-9177.

Kristensen L.S., Andersen M.S., Stagsted L.V.W., Ebbesen K.K., Hansen T.B. and Kjems J. (2019). The biogenesis, biology and characterization of circular RNAs. Nat. Rev. Genet. 20, 675-691.

Kurita K., Maeda M., Mansour M.A., Kokuryo T., Uehara K., Yokoyama Y., Nagino M., Hamaguchi M. and Senga T. (2016). TRIP13 is expressed in colorectal cancer and promotes cancer cell invasion. Oncol. Lett. 12, 5240-5246.

Lin J., Shi Z., Yu Z. and He Z. (2018). LncRNA HIF1A-AS2 positively affects the progression and EMT formation of colorectal cancer through regulating miR-129-5p and DNMT3A. Biomed. Pharmacother. 98, 433-439.

Lu J.L., Zhao L., Han S.C., Bi J.L., Liu H.X., Yue C. and Lin L. (2018). MiR-129 is involved in the occurrence of uterine fibroid through inhibiting TET1. Eur. Rev. Med. Pharmacol. Sci. 22, 4419-4426.

Lu S., Guo M., Fan Z., Chen Y., Shi X., Gu C. and Yang Y. (2019a). Elevated TRIP13 drives cell proliferation and drug resistance in bladder cancer. Am. J. Transl. Res. 11, 4397-4410.

Lu S., Qian J., Guo M., Gu C. and Yang Y. (2019b). Insights into a Crucial Role of TRIP13 in Human Cancer. Comput. Struct. Biotechnol. J. 17, 854-861.

Lu T.X. and Rothenberg M.E. (2018). MicroRNA. J. Allergy Clin. Immunol. 141, 1202-1207.

Mauri G., Sartore-Bianchi A., Russo A.G., Marsoni S., Bardelli A. and

Siena S. (2019). Early-onset colorectal cancer in young individuals. Mol. Oncol. 13, 109-131.

Mishra S., Yadav T. and Rani V. (2016). Exploring miRNA based approaches in cancer diagnostics and therapeutics. Crit. Rev. Oncol. Hematol. 98, 12-23.

Rupaimoole R. and Slack F.J. (2017). MicroRNA therapeutics: towards a new era for the management of cancer and other diseases. Nat. Rev. Drug. Discov. 16, 203-222.

Setijono S.R., Park M., Kim G., Kim Y., Cho K.W. and Song S.J. (2018). miR-218 and miR-129 regulate breast cancer progression by targeting Lamins. Biochem. Biophys. Res. Commun. 496, 826-833.

Sheng N., Yan L., Wu K., You W., Gong J., Hu L., Tan G., Chen H. and Wang Z. (2018). TRIP13 promotes tumor growth and is associated with poor prognosis in colorectal cancer. Cell Death Dis. 9, 402.

Takahashi R.U., Prieto-Vila M., Kohama I. and Ochiya T. (2019). Development of miRNA-based therapeutic approaches for cancer patients. Cancer Sci. 110, 1140-1147.

Tiwari A., Mukherjee B. and Dixit M. (2018). MicroRNA Key to Angiogenesis Regulation: MiRNA Biology and Therapy. Curr. Cancer Dru. Targets 18, 266-277.

Vader G. (2015). Pch2(TRIP13): controlling cell division through regulation of HORMA domains. Chromosoma 124, 333-339.

Wang K., Sturt-Gillespie B., Hittle J.C., Macdonald D., Chan G.K., Yen T.J. and Liu S.T. (2014). Thyroid hormone receptor interacting protein 13 (TRIP13) AAA-ATPase is a novel mitotic checkpoint-silencing protein. J. Biol. Chem. 289, 23928-23937.

Wu Q., Meng W.Y., Jie Y. and Zhao H. (2018). LncRNA MALAT1 induces colon cancer development by regulating miR-129-5p/HMGB1 axis. J. Cell Physiol. 233, 6750-6757.

Yuan C. and Yang L. (2020). Long non-coding RNA PITPNA-AS1 accelerates the progression of colorectal cancer through miR-129-5p/HMGB1 axis. Cancer Manag. Res. 12, 12497-12507.

Zhang G., Zhu Q., Fu G., Hou J., Hu X., Cao J., Peng W., Wang X., Chen F. and Cui H. (2019a). TRIP13 promotes the cell proliferation, migration and invasion of glioblastoma through the FBXW7/c-MYC axis. Br. J. Cancer 121, 1069-1078.

Zhang Q., Dong Y., Hao S., Tong Y., Luo Q. and Aerxiding P. (2019b). The oncogenic role of TRIP13 in regulating proliferation, invasion, and cell cycle checkpoint in NSCLC cells. Int. J. Clin. Exp. Pathol. 12, 3357-3366.

Zhou X.Y. and Shu X.M. (2019). TRIP13 promotes proliferation and invasion of epithelial ovarian cancer cells through Notch signaling pathway. Eur. Rev. Med. Pharmacol. Sci. 23, 522-529.

Accepted April 1, 2022